

Implementation and Performance Analyses of a Highly Efficient Algorithm for Pressure-Velocity Coupling

Implementierung und Untersuchung einer hoch effizienten Methode zur
Druck-Geschwindigkeits-Kopplung
Master-Thesis von Fabian Gabel
Tag der Einreichung:

1. Gutachten: Prof. Dr. rer. nat. Michael Schäfer
2. Gutachten: Dipl.-Ing Ulrich Falk



TECHNISCHE
UNIVERSITÄT
DARMSTADT

Studienbereich CE
FNB

Implementation and Performance Analyses of a Highly Efficient Algorithm for Pressure-Velocity Coupling
Implementierung und Untersuchung einer hoch effizienten Methode zur Druck-Geschwindigkeits-Kopplung

Vorgelegte Master-Thesis von Fabian Gabel

1. Gutachten: Prof. Dr. rer. nat. Michael Schäfer
2. Gutachten: Dipl.-Ing Ulrich Falk

Tag der Einreichung:

Erklärung zur Master-Thesis

Hiermit versichere ich, die vorliegende Master-Thesis ohne Hilfe Dritter nur mit den angegebenen Quellen und Hilfsmitteln angefertigt zu haben. Alle Stellen, die aus Quellen entnommen wurden, sind als solche kenntlich gemacht. Diese Arbeit hat in gleicher oder ähnlicher Form noch keiner Prüfungsbehörde vorgelegen.

Darmstadt, den 20. Januar 2015

(F. Gabel)

Contents

1	Introduction	3
2	Fundamentals of Continuum Physics for Thermo-Hydrodynamical Problems	4
2.1	Conservation of Mass – Continuity Equation	4
2.2	Conservation of Momentum – Cauchy-Equations	4
2.3	Closing the System of Equations – Newtonian Fluids	5
2.4	Conservation Law for Scalar Quantities	5
2.5	Necessary Simplification of Equations	5
2.5.1	Incompressible Flows and Hydrostatic Pressure	6
2.5.2	Variation of Fluid Properties – The Boussinesq Approximation	6
2.6	Final Form of the Set of Equations	7
3	Finite Volume Method for Incompressible Flows – Theoretical Basics	8
3.1	Numerical Grid	8
3.2	Approximation of Integrals and Derivatives	9
3.3	Treatment of Non-Orthogonality of Grid Cells	10
3.3.1	Minimum Correction Approach	10
3.3.2	Orthogonal Correction Approach	10
3.3.3	Over-Relaxed Approach	10
3.3.4	Deferred Non-Orthogonal Correction	10
3.4	Numerical Solution of Non-Linear Systems – Linearization Techniques	11
3.5	Numerical Solution of Linear Systems	11
3.5.1	Stone’s SIP Solver	11
3.5.2	Krylov Subspace Methods	11
4	Implicit Finite Volume Method for Incompressible Flows – Segregated Approach	12
4.1	Calculation of Mass Fluxes and the Pressure-Weighted Interpolation Method	12
4.2	Implicit Pressure Correction and the SIMPLE Algorithm	13
4.3	Discretization of the Momentum Balance	15
4.3.1	Linearization and Discretization of the Convective Term	15
4.3.2	Discretization of the Diffusive Term	16
4.3.3	Discretization of the Source Terms	17
4.4	Discretization of the Pressure Correction Equation	17
4.5	Discretization of the Temperature Equation	17
4.6	Boundary Conditions	18
4.7	Structure of the Assembled Linear Systems	18
5	Finite Volume Method for Incompressible Flows – Coupled Approach	20
5.1	The Coupled Algorithm	20
5.1.1	Pressure Equation	20
5.1.2	Characteristic Properties of Coupled Solution Methods	20
5.2	Coupling the Temperature Equation	20
5.2.1	Decoupled Approach	20
5.2.2	Velocity-Temperature Coupling	20
5.2.3	Temperature-Velocity/Pressure Coupling – Newton-Raphson Linearization	20
5.3	Boundary Conditions on Domain and Block Boundaries	20
5.3.1	Dirichlet Boundary Condition for Velocity	20
5.3.2	Wall Boundary Condition	20
5.3.3	Block Boundary Condition	20
5.4	Assembly of Linear Systems – Final Form of Equations	20
6	CAFFA Framework	21
6.1	PETSc Framework	21
6.1.1	About PETSc	21
6.1.2	Basic Data Types	21
6.1.3	KSP and PC Objects and Their Usage	21

6.1.4	Profiling	21
6.1.5	Common Errors	21
6.2	Grid Generation and Conversion	21
6.3	Preprocessing	21
6.4	Implementation Details of CAFFA	21
6.4.1	MPI Programming Model	21
6.4.2	Convergence Control	22
6.4.3	Modi of Calculation	22
6.4.4	Indexing of Variables and Treatment of Boundary Values	22
6.4.5	Field Interlacing	22
6.4.6	Domain Decomposition, Exchange of Ghost Values and Parallel Matrix Assembly	22
6.5	Postprocessing	22
7	Verification of the developed CAFFA Framework	23
7.1	Theoretical Discretization Error	23
7.2	Method of Manufactured Solutions	23
7.3	Exact and Manufactured Solutions for the Navier-Stokes Equations and the Energy Equation	23
7.4	Measurement of Error and Calculation of Order	23
7.4.1	Testcase on Single Processor on Orthogonal Locally Refined Grid	23
7.4.2	Testcase on Multiple Processors on Non-Orthogonal Locally Refined Grid	23
8	Comparison of Solver Concepts	24
8.1	Convergence Behaviour on Locally Refined Block Structured Grids with Different Degrees of Coupling . . .	24
8.2	Parallel Performance	24
8.2.1	Employed Hardware and Software – The Lichtenberg-High Performance Computer	24
8.2.2	Measures of Performance	24
8.2.3	Preliminary Upper Bounds on Performance – The STREAM Benchmark	24
8.2.4	Discussion of Results for Parallel Efficiency	24
8.2.5	Speedup Measurement for Analytic Test Cases	24
8.3	Test Cases with Varying Degree of Non-Linearity	24
8.3.1	Transport of a Passive Scalar – Forced Convection	24
8.3.2	Buoyancy Driven Flow – Natural Convection	24
8.3.3	Flow with Temperature Dependent Density – A Highly Non-Linear Test Case	24
8.4	Realistic Testing Scenarios – Benchmarking	24
8.4.1	Flow Around a Cylinder 3D – Stationary	25
8.4.2	Flow Around a Cylinder 3D – Instationary	25
8.4.3	Heat-Driven Cavity Flow	25
8.5	Realistic Testing Scenario – Complex Geometry	25
9	Conclusion and Outlook	26
	References	27

List of Figures

1	Comparison of vertex oriented and cell center oriented variable arrangement	8
2	Block structured grid consisting of two blocks	9
3	Minimum correction, orthogonal correction and over-relaxed approach	11

List of Tables

List of Algorithms

1	SIMPLE Algorithm	15
---	----------------------------	----

1 Introduction

This thesis is about.

2 Fundamentals of Continuum Physics for Thermo-Hydrodynamical Problems

This section covers the set of fundamental equations for thermo-hydrodynamical problems which the numerical solution techniques of the following chapters are aiming to solve. Furthermore the notation regarding the physical quantities to be used throughout this thesis is introduced. The following paragraphs are based on (Kundu, Spurk, Ferziger, Anderson). For a thorough derivation of the matter to be presented the reader may consult the mentioned sources. Since the present thesis focusses on the application of finite-volume methods the focus lays on stating the integral forms of the relevant conservation laws. However in the process of deriving the final set of equations the use of differential formulations of the stated laws are required. Einstein's convention for taking sums over repeated indices is used to simplify certain expressions. For the remainder of this thesis non-moving inertial frames in a Cartesian coordinate system with the coordinates x_i are used. This approach is also known as *Eulerian approach*.

2.1 Conservation of Mass – Continuity Equation

The conservation law of mass embraces the physical concept that, neglecting relativistic and nuclear reactions, mass cannot be created or destroyed. Using the notion of a mathematical control volume, which is used to denote a constant domain of integration, one can state the integral mass balance of a control volume V with control surface S with surface normal unit vector $\mathbf{n} = (n_i)_{i=1,\dots,3}$ using Gauss' theorem as

$$\iiint_V \frac{\partial \rho}{\partial t} + \frac{\partial}{\partial x_i} (\rho u_i) dV = \iiint_V \frac{\partial \rho}{\partial t} dV + \iint_S \rho u_i n_i dS = 0,$$

where ρ denotes the material density, t denotes the independent variable of time and $\mathbf{u} = (u_i)_{i=1,\dots,3}$ is the velocity vector field. Since this equation remains valid for arbitrary control volumes the equality has to hold for the integrands as well. In this sense the differential form of the conservation law of mass can be formulated as

$$\frac{\partial \rho}{\partial t} + \frac{\partial}{\partial x_i} (\rho u_i) = 0. \quad (1)$$

2.2 Conservation of Momentum – Cauchy-Equations

The conservation law of momentum, also known as Newton's Second Law, axiomatically demands the balance of the temporal change of momentum and the sum of all attacking forces on a body. Those forces can be divided into body forces and surface forces. Let $\mathbf{k} = (k_i)_{i=1,\dots,3}$ denote a mass specific force and $\mathbf{t} = (t_i)_{i=1,\dots,3}$ the stress vector. A first form of the integral momentum balance in the direction of x_i can be formulated as

$$\iiint_V \frac{\partial (\rho u_i)}{\partial t} dV + \iint_S \rho u_i (u_j n_j) dS = \iiint_V \rho k_i dV + \iint_S t_i dS.$$

In general the stress vector \mathbf{t} is a function not only of the location $\mathbf{x} = (x_i)_{i=1,\dots,3}$ and of the time t but also of the surface normal unit vector \mathbf{n} . A central simplification can be introduced, namely Cauchy's stress theorem, which states that the stress vector is the image of the normal vector under a linear mapping \mathbf{T} . With respect to the Cartesian canonical basis $(\mathbf{e}_i)_{i=1,\dots,3}$ the mapping \mathbf{T} is represented by the coefficient matrix $(\tau_{ji})_{i,j=1,\dots,3}$ and Cauchy's stress theorem reads

$$\mathbf{t}(\mathbf{x}, t, \mathbf{n}) = \mathbf{T}(\mathbf{x}, t, \mathbf{n}) = (\tau_{ji} n_j)_{i=1,\dots,3}.$$

Assuming the validity of Cauchy's stress theorem one can derive Cauchy's first law of motion, which in differential form can be formulated as

$$\frac{\partial (\rho u_i)}{\partial t} + \frac{\partial}{\partial x_j} (\rho u_i u_j) = \rho k_i + \frac{\partial \tau_{ji}}{\partial x_j} \quad (2)$$

and represents the starting point for the modelling of fluid mechanical problems. One should note, that Cauchy's first law of motion does not take any assumptions regarding material properties, which is why the set of equations (1,2) is not closed in the sense that there exists a independent equation for each of the dependent variables.

2.3 Closing the System of Equations – Newtonian Fluids

As result of Cauchy's theorem the stress vector \mathbf{t} can be specified once the nine components τ_{ji} of the coefficient matrix are known. As is shown in (Spurk usw.) by formulating the conservation law of angular momentum the coefficient matrix is symmetric,

$$\tau_{ji} = \tau_{ij}, \quad (3)$$

hence the number of unknown coefficients may be reduced to six unknown components. In a first step it is assumed that the coefficient matrix can be decomposed into fluid-static and fluid-dynamic contributions,

$$\tau_{ij} = -p\delta_{ij} + \sigma_{ij},$$

where p is the thermodynamic pressure, δ_{ij} is the *Kronecker-Delta* and σ_{ij} is the so called *deviatoric stress tensor*.

For the fluids the studies that the present thesis performs it is sufficient to consider viscous fluids for which there exists a linear relation between the components of the deviatoric stress tensor and the symmetric part of the transpose of the jacobian of the velocity field $(S_{ij})_{i,j=1,\dots,3}$,

$$S_{ij} = \frac{1}{2} \left(\frac{\partial u_i}{\partial x_j} + \frac{\partial u_j}{\partial x_i} \right).$$

If one now imposes material-isotropy and the mentioned stress-symmetry (3) restriction it can be shown (Aries) that the constitutive equation for the deviatoric stress tensor reads

$$\sigma_{ij} = 2\mu S_{ij} + \lambda S_{mm} \delta_{ij},$$

where λ and μ denominate scalars which depend on the local thermodynamical state. Taking everything into account (2) can be formulated as the differential conservation law of momentum for newtonian fluids, better known as the *Navier-Stokes equations* in differential form:

$$\frac{\partial (\rho u_i)}{\partial t} + \frac{\partial}{\partial x_j} (\rho u_i u_j) = \rho k_i - \frac{\partial p}{\partial x_i} + \frac{\partial}{\partial x_j} \left(\mu \left(\frac{\partial u_i}{\partial x_j} + \frac{\partial u_j}{\partial x_i} \right) \right) + \frac{\partial}{\partial x_i} \left(\lambda \frac{\partial u_m}{\partial x_m} \right) \quad (4)$$

2.4 Conservation Law for Scalar Quantities

The modelling of the transport of scalar quantities, convection, by a flow field \mathbf{u} is necessary if the fluid mechanical problem to be analyzed includes for example heat transfer. Other scenarios that involve the necessity to model scalar transport surge, when turbulent flows are to be modeled by two-equation models like the k - ε -model (REFERENCE,Pope).

Since this thesis focusses on the transport of the scalar temperature T this section introduces the conservation law for energy in differential form,

$$\frac{\partial (\rho T)}{\partial t} + \frac{\partial}{\partial x_j} \left(\rho u_j T - \kappa \frac{\partial T}{\partial x_j} \right) = q_T, \quad (5)$$

where κ denotes the thermal conductivity of the modelled material and q_T is a scalar field representing sources and sinks of heat throughout the domain of the problem.

2.5 Necessary Simplification of Equations

Negligible viscous dissipation and pressure work source terms in the enery equation (vakilipour)

The purpose of this section is to motivate and introduce further common simplifications of the previously presented set of constitutive equations.

2.5.1 Incompressible Flows and Hydrostatic Pressure

A common simplification when modelling low Mach number flows ($Ma < 0.3$), is the assumption of *incompressibility*, or the assumption of an *isochoric* flow. If one furthermore assumes homogeneous density ρ in space and time, a restrictive assumption that will be partially alleviated in the following section the continuity equation in differential form (1) can be simplified to

$$\frac{\partial u_i}{\partial x_i} = 0. \quad (6)$$

In other words: In order for a velocity vector field \mathbf{u} to be valid for an incompressible flow it has to be free of divergence, or *solenoidal* (Aries).

If furthermore, one assumes also constant dynamic viscosity μ , which can be suitable in the case of isothermal flow or if the temperature differences within the flow are small, the Navier-Stokes equations in differential form can be reduced to

$$\frac{\partial (\rho u_i)}{\partial t} + \rho \frac{\partial}{\partial x_j} (u_i u_j) = \rho k_i - \frac{\partial p}{\partial x_i} + \frac{\partial}{\partial x_j} \left(\mu \left(\frac{\partial u_i}{\partial x_j} + \frac{\partial u_j}{\partial x_i} \right) \right) \quad (7a)$$

$$= \rho k_i - \frac{\partial p}{\partial x_i} + \mu \frac{\partial}{\partial x_j} \left(\frac{\partial u_i}{\partial x_j} \right) \quad (7b)$$

by using *Schwartz's* lemma to interchange the order of differentiation. A common simplification to further simplify the set of equations is the assumption of a volume specific force $\rho \mathbf{k}$ that can be modelled by a potential, such that it can be represented as the gradient of a scalar field $\Phi_{\mathbf{k}}$ as

$$-\rho k_i = \frac{\partial \Phi_{\mathbf{k}}}{\partial x_i}.$$

In the case of this thesis this assumption is valid since the mass specific force is the mass specific gravitational force $\mathbf{g} = (g_i)_{i=1,\dots,3}$ and the density is assumed to be constant, so the potential can be modelled as

$$\Phi_g = -\rho g_j x_j.$$

This term can be interpreted as the hydrostatic pressure p_{hyd} and can be added to the thermodynamical pressure p to simplify calculations

$$\begin{aligned} \rho g_i - \frac{\partial p}{\partial x_i} &= \frac{\partial}{\partial x_i} (\rho g_j x_j) - \frac{\partial p}{\partial x_i} \\ &= \frac{\partial}{\partial x_i} (\rho g_j x_j) - \frac{\partial}{\partial x_i} (\hat{p} + p_{hyd}) \\ &= -\frac{\partial \hat{p}}{\partial x_i}. \end{aligned} \quad (8)$$

Since in incompressible fluids only pressure differences matter, this has no effect on the solution. After finishing the calculations p_{hyd} can be calculated and added to the resulting pressure \hat{p} .

2.5.2 Variation of Fluid Properties – The Boussinesq Approximation

If modelling of an incompressible flow involves heat transfer fluid properties like the density change with varying temperature. If the variation of temperature is small one can still assume a constant density to maintain the structure of the advection and diffusion terms in (4) and only consider the changes of the density in the gravitational term. If linear variation of density with respect to temperature is assumed this approximation is called *Boussinesq*-approximation. In this case the Navier-Stokes equations are formulated using a reference pressure ρ_0 at the reference temperature T_0 and the now temperature dependent density ρ , with

$$\rho(T) = \rho_0 (1 - \beta (T - T_0)). \quad (9)$$

Here β denotes the coefficient of thermal expansion. Under the use of the Boussinesq-approximation the incompressible Navier-Stokes equations in differential form can be formulated as

$$\begin{aligned}
\rho_0 \frac{\partial (u_i)}{\partial t} + \rho_0 \frac{\partial}{\partial x_j} (u_i u_j) &= \rho_0 g_i + (\rho - \rho_0) g_i - \frac{\partial p}{\partial x_i} + \mu \frac{\partial}{\partial x_j} \left(\frac{\partial u_i}{\partial x_j} + \frac{\partial u_j}{\partial x_i} \right) \\
&= \frac{\partial}{\partial x_i} (\rho_0 g_j x_j) + (\rho - \rho_0) g_i - \frac{\partial p}{\partial x_i} + \mu \frac{\partial}{\partial x_j} \left(\frac{\partial u_i}{\partial x_j} + \frac{\partial u_j}{\partial x_i} \right) \\
&= - \frac{\partial \hat{p}}{\partial x_i} + (\rho - \rho_0) g_i + \mu \frac{\partial}{\partial x_j} \left(\frac{\partial u_i}{\partial x_j} + \frac{\partial u_j}{\partial x_i} \right) \\
&= - \frac{\partial \hat{p}}{\partial x_i} - \rho_0 \beta (T - T_0) + \mu \frac{\partial}{\partial x_j} \left(\frac{\partial u_i}{\partial x_j} + \frac{\partial u_j}{\partial x_i} \right)
\end{aligned}$$

using ρg as the mass specific force.

- Talk about natural and forced convection. Differences for the solver algorithm. (s.a.) Peric P447
- Talk about flows with variation in fluid properties -> mms has to map this behaviour (Buoyancy force driven, i.e. naturally convected fluid), mixed Convection
- Also talk about non-dimensional values like Prandtl number, Rayleigh and Reynolds
- Talk about the validity of this approximation

2.6 Final Form of the Set of Equations

In the previous subsections different simplifications have been introduced which will be used throughout the thesis. The final form of the set of equations to be used is thereby presented. As further simplification the modified pressure \hat{p} will be treated as p and since the use of the Boussinesq-approximation substitutes the variable ρ by a linear function of the temperature T the reference pressure ρ_0 for the remainder of this thesis will be referred to as ρ . Note that incompressibility has been taken into account:

$$\frac{\partial u_i}{\partial x_i} = 0. \quad (10a)$$

$$\rho \frac{\partial (u_i)}{\partial t} + \rho \frac{\partial}{\partial x_j} (u_i u_j) = - \frac{\partial p}{\partial x_i} - \rho \beta (T - T_0) + \mu \frac{\partial}{\partial x_j} \left(\frac{\partial u_i}{\partial x_j} + \frac{\partial u_j}{\partial x_i} \right) \quad (10b)$$

$$\frac{\partial (\rho T)}{\partial t} + \frac{\partial}{\partial x_j} \left(\rho u_j T - \kappa \frac{\partial T}{\partial x_j} \right) = q_T. \quad (10c)$$



Figure 1: Comparison of vertex oriented and cell center oriented variable arrangement

3 Finite Volume Method for Incompressible Flows – Theoretical Basics

This section deals with the fundamentals of the numerical solution via a finite volume method of the formerly presented set of partial differential equations. The focus of this section is, to provide an overview over the methods to be used in the present thesis. The information contained in this section is based on (Peric, Schäfer, Muzaferja, Jsak). The overview starts by mentioning the different grid types to be used and the discretization techniques to be applied. On the basis of integral formulations of the equations to be solved, the therein contained integrals and differential operators have to be discretized. Since the accuracy of the default concepts for discretizing differential operators degrades with decreasing grid quality, this chapter furthermore presents different approaches to handle corrections for cases in which the cause of degrading grid quality is increased non-orthogonality.

The goal of the finite volume method is to provide algebraic equations which can be used to determine an approximate solution of a partial differential equation. This system of linear algebraic equations can be solved by means of algorithms to be presented in the end of this section. However since the Navier-Stokes equations are in general non-linear an intermediate step has to be taken, by linearizing the discrete equations. This leads to the need of an iteration process, the *Picard iteration*, which will be explained briefly.

3.1 Numerical Grid

In this subsection a brief overview of the general grid structure to be used in the present thesis is given. The main idea behind finite volume methods is to solve partial differential equations by integrating them over the specified continuous problem domain and dividing this domain into a finite number of subdomains, the so called control volumes. The result of this finite partition of a continuous problem domain is called the numerical grid. The grid consists of a finite number of grid cells which represent the boundaries of a discrete domain of integration. Depending on whether the numerical solution of an equation is to be calculated on the boundary vertices of grid cell or in the center of the cell, the variable arrangement is denoted to be vertex or cell center oriented. As the methods employed in the present thesis are intended to be generally applicable to complex geometries the cell centered approach offers more flexibility (3.1). DONT CONFUSE WITH STAGGERED AND COLLOCATED ARRANGEMENT.

Regarding the treatment of domain boundaries and the ordering of the cells within the problem domain different types of numerical grids can be distinguished. The present thesis makes use of so called block structured grids with hexahedron cells. A structured grid is characterized by a constant amount of grid cells in each coordinate direction. The high regularity of structured grids benefits the computational efficiency of algorithms to be used on this type of grid. A block structured grid consists of different grid blocks of which each considered individually is structured, but if the topology of the grid is considered it is unstructured. An example of a block structured grid with distinguishable grid blocks is given in figure 3.1. The use of block structured grids is motivated by the need to increase the adaptivity of structured grids by maintaining high computational efficiency. Furthermore it naturally embraces the concept of domain decomposition which facilitates the implementation of parallel algorithms for the decomposed computational domain.

Inside a structured grid block, cells with the shape of hexahedrons are used. In addition to the geometric boundaries of each control volume a numerical grid also provides a mapping that assigns to each control volume with index P a set of indexes of neighbouring control volumes $NB(P) := \{W, S, B, T, N, E\}$, which are named after the geographic directions. Figure 3.1 shows a single grid cell with its direct neighbours. The faces $\{S_w, S_s, S_b, S_t, S_n, S_e\}$ of each hexahedral control volume represent the mentioned geometric boundaries.

- talk about grid quality
- talk about local refinement

- talk about variable arrangement

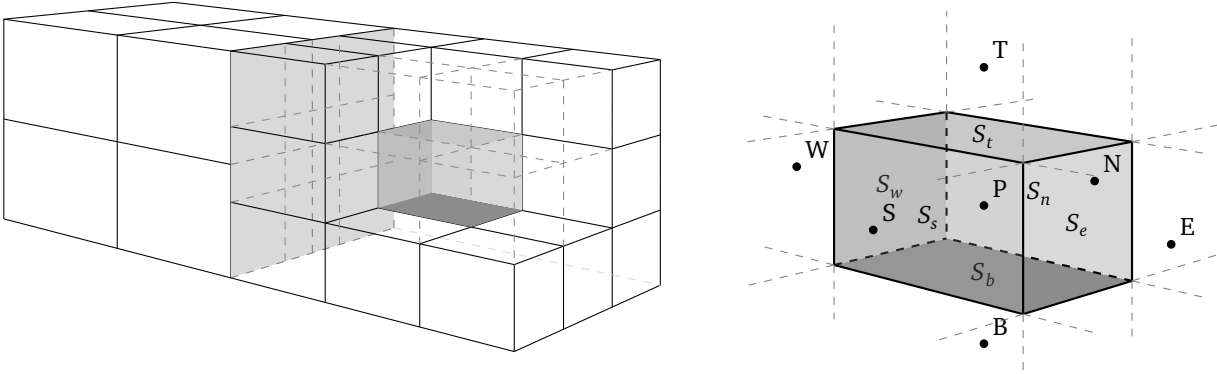


Figure 2: Block structured grid consisting of two blocks

3.2 Approximation of Integrals and Derivatives

In the course of transforming a partial differential equation into a system of linear algebraic equations, integrals and derivatives have to be approximated. The simplest method for approximating an integral is by using the *midpoint rule*. This rule is similar to the mean value theorem of integration, which states that there exists a point $\xi \in V$ for a Riemann integrable function ϕ such that $\phi(\xi) \int_V dV = \int_V \phi(x) dV$. For the midpoint rule ξ is taken to be the center of mass of V . If the integration domain V is indeed a Volume, fortunately the calculation of $\phi(\xi)$ with $\xi := (\int_V x_i dV / \int_V dV)_{i=1,\dots,3}$ presents no difficulties since due to the collocated variable arrangement the value of ϕ is stored in the cell center, which corresponds to the location ξ . However if the domain of integration is a surface, a preceding interpolation step is necessary.

On the other hand to transform a partial differential equation into a linear algebraic equation it is necessary to discretize the differential operators of the equations. For numerical reasons two different discretization techniques are used in this thesis. A common task is to discretize expressions of the form

$$(\nabla \phi)_e \cdot \mathbf{n}_e,$$

where $(\nabla \phi)_e$ is the Gradient of ϕ on a boundary face S_e . One method is to directly interpret this expression as a directional derivative and approximate it with a central difference

$$(\nabla \phi)_e \cdot \mathbf{n}_e \approx \frac{\phi_P - \phi_E}{\|\mathbf{x}_P - \mathbf{x}_E\|_2}. \quad (11)$$

Another method would be to first calculate the cell center gradients $(\nabla \phi)_P$ and $(\nabla \phi)_E$ and interpolate them linearly before calculating the projection onto \mathbf{n}_e

$$(\nabla \phi)_e \cdot \mathbf{n}_e \approx [\gamma_e (\nabla \phi)_P + (1 - \gamma_e) (\nabla \phi)_E] \cdot \mathbf{n}_e, \quad (12)$$

where $\gamma_e := \|\mathbf{x}_P - \mathbf{x}_e\|_2 / \|\mathbf{x}_P - \mathbf{x}_E\|_2$ is a geometric interpolation factor. For calculating the cell center gradients a method based on Gauss' integration theorem and the midpoint rule for volume integration is employed

$$(\nabla \phi)_{i,P} = \left(\frac{\partial \phi}{\partial x_i} \right)_P \approx \frac{\int_V \left(\frac{\partial \phi}{\partial x_i} \right)_P dV}{|V|}. \quad (13)$$

Briefly explain the idea behind the quadrature via the midpoint rule. Talk about central differences and the approximation via the gauss theorem. Maybe talk about the resulting order of the truncation error.

3.3 Treatment of Non-Orthogonality of Grid Cells

Unfortunately real applications involve complex geometries, which in turn affects the orthogonality of the grid. On non-orthogonal meshes the directional derivative in direction of the face normal unit vector \mathbf{n}_e can no longer be approximated as in (11). On the other side the exclusive usage of (13) is not desirable due to the bigger truncation error that comes with this approximation (PROOF?). Hence a compromise is made and the surface vector $\mathbf{S}_e := S_e \mathbf{n}_e$ is decomposed as

$$\mathbf{S}_e = \Delta + \mathbf{k}, \quad (14)$$

where Δ is parallel to the vector $\mathbf{d}_e := (\mathbf{x}_E - \mathbf{x}_P)$ that directly connects the center of the control volume P with the center of its neighbour E . This vector controls the *orthogonal* contribution to the directional derivative. The vector \mathbf{k} controls the influence of the *non-orthogonal* contribution. In the next paragraphs the three main decompositions of the surface vector \mathbf{S}_e will be presented by stating the respective expression for Δ . The resulting vector \mathbf{k} can be calculated by using (14). One important characteristic that all of the presented approaches have is common is that the non-orthogonal contribution vanishes as expected, when an orthogonal grid is used. For simplicity the presentation of the decompositions is chosen to be two dimensional. An geometrical interpretation of the three approaches is given in 3.3.3. The last subsection handles the integration of one generic approach into the discretization process.

3.3.1 Minimum Correction Approach

This is the approach as proposed in Muzaferja. The reader should note, that even though Ferziger/Peric reference the work of Muzaferja they use a different approach to be presented in the next paragraph. This method is designed to keep the non-orthogonal contribution minimal by always choosing \mathbf{k} to be orthogonal to Δ , which leads to

$$\Delta = (\mathbf{d} \cdot \mathbf{S}_e) \frac{\mathbf{d}}{\|\mathbf{d}\|_2}.$$

It should be noted that the Influence of the orthogonal contribution decreases with increasing non-orthogonality of the grid.

3.3.2 Orthogonal Correction Approach

The following method for decomposing the surface normal vector is presented in Ferziger/Peric and the approach implemented in the developed solvers. In this approach a simple projection is used which is independent of the non-orthogonality of the grid. As a result the orthogonal contribution $\|\Delta\|_2 = \|\mathbf{S}_e\|_2$ and is thus modelled as

$$\Delta = S_e \frac{\mathbf{d}}{\|\mathbf{d}\|_2}.$$

3.3.3 Over-Relaxed Approach

The last approach is used in Jsak and Darwish and is characterized by an increasing influence of the orthogonal contribution with increasing grid non-orthogonality, as opposed to the minimum correction approach. The orthogonal contribution is calculated as

$$\Delta = S_e^2 \frac{\mathbf{d}}{\mathbf{d} \cdot \mathbf{S}_e}.$$

3.3.4 Deferred Non-Orthogonal Correction

In order to reduce the computational stencil that would be necessary to handle the non-orthogonal correction implicitly the correction will be treated explicitly using a deferred correction which guarantees that in the case of a fully converged solution only the face normal derivative has been taken into account. Generally the discretization using a non-orthogonal correction would yield

$$(\nabla \phi)_e \cdot \mathbf{S}_e \approx (\nabla \phi)_e \cdot \Delta + (\nabla \phi)_e \cdot \mathbf{k}.$$

Where the first term can be approximated using a central differencing scheme for the directional derivative and the second by interpolating cell center gradients. If one furthermore uses the fact that this method comes to play in an solution algorithm for a non-linear system of partial differential equations a deferred correction can be implemented which ensues a smaller error from the non-orthogonality. In the case of the previously mentioned discretization techniques for partial derivatives a possible deferred correction approach reads

$$(\nabla \phi)_e \cdot \mathbf{S}_e \approx \|\Delta\|_2 \frac{\phi_P - \phi_E}{\|\mathbf{x}_P - \mathbf{x}_E\|_2} - (\nabla \phi)_e^{(n-1)} \cdot (\Delta - \mathbf{S}_e).$$

It should be noted that the use of a deferred correction in conjunction with the requirement that the non-orthogonal correction vanishes on orthogonal grid introduces an inconsistent discretization of $(\nabla \phi)_e \cdot \Delta$.

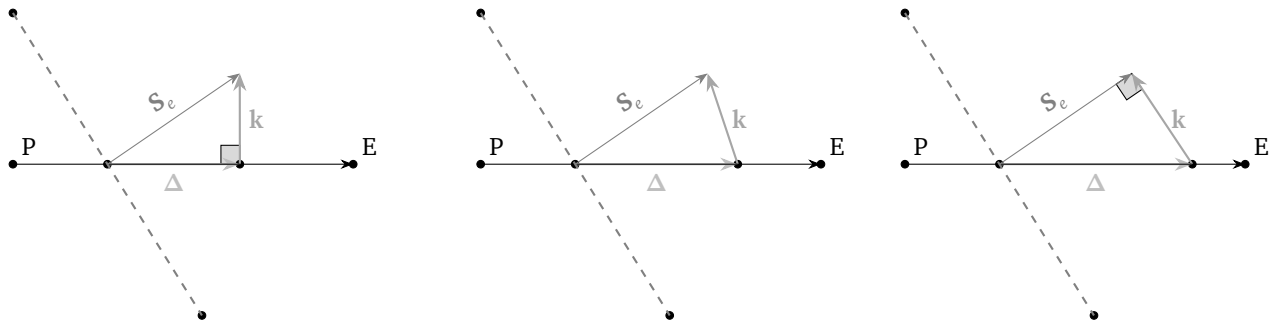


Figure 3: Minimum correction, orthogonal correction and over-relaxed approach

3.4 Numerical Solution of Non-Linear Systems – Linearization Techniques

Introduce the concept of the Picard-Iteration as a linearization technique. Introduce the notions of inner and outer iterations. Refer to later chapters when it comes to deferred correction.

3.5 Numerical Solution of Linear Systems

3.5.1 Stone's SIP Solver

Basic Idea as in Schäfer or Peric. Emphasize that this is a very problem specific approach, that cannot be generalized that easily in opposition to the general purpose linear solvers from PETSc. Present either BiCGStab or GMRES, the one which performs better and is used throughout the thesis.

3.5.2 Krylov Subspace Methods

- General concept of cyclic vector spaces of \mathbb{R}^n ,
- talk about bases of krylov subspaces and the arnoldi algorithm, talk about polynomials and linear combinations
- mention the two major branches (minimum residual approach, petrov and ritz-galerkin approach)
- name some representative ksp algorithms, importance of preconditioning, not as detailed as in bachelor thesis
- in cases there is a nonempty Nullspace what happens?

4 Implicit Finite Volume Method for Incompressible Flows – Segregated Approach

The purpose of this section is to present the discretization applied to the set of equations (10). Since the system of partial differential equations to be solved always exhibits a coupling at least between the dependent variables pressure and velocity a first solution algorithm, namely the *SIMPLE* algorithm addressed to resolve the pressure velocity coupling is introduced. Methods of calculating mass fluxes and the detailed derivation of all coefficients that result from the discretization process is presented. The discretization of those boundary conditions, that are relevant for the present thesis will be presented in their own subsection.

4.1 Calculation of Mass Fluxes and the Pressure-Weighted Interpolation Method

The advantages of using a cell-centered variable arrangement are evident: The treatment of non-orthogonality is simplified and the conservation property of finite volume methods is retained [5, 17, 18, 27]. A major drawback if *SIMPLE*-Type algorithms, to be introduced in section 4.2, are used is that pressure field may delink which will then lead to unphysical oscillations in both the pressure and the velocity results. This . If the oscillations are severe enough the solution algorithm might get unstable and diverge. The described decoupling occurs, when the pressure gradient in the momentum balances and the mass fluxes in the continuity equation are discretized using central differences. A common practice to eliminate this behaviour is the use of a momentum interpolation technique, also known as *Rhie-Chow Interpolation* [21]. The original interpolation scheme however doesn't guarantee a unique solution, independent of the amount of under-relaxation. The performance of one of the algorithms that are used in the present thesis heavily relies on the under-relaxation of variables to accomplish stability. Furthermore the original method as proposed by [21] does not account for large body forces which also may lead to unphysical results. This issues will be addressed in this subsection which at the end will present an interpolation method that assures an under-relaxation independent solution, the *pressure-weighted interpolation method* [18].

Starting point of the pressure-weighted interpolation method are the discretized momentum balances at node P and the neighbouring node Q . The discretization for a finite volume methods and details including the incorporation of under-relaxation factors will be handled in subsection 4.3. The semi-discrete implicit momentum balances read if one solves for the velocity at node P or Q

$$u_{i,P}^{(n)} = -\frac{\alpha_{u_P}}{a_{P,u_i}} \left(\sum_{F \in NB(P)} a_{F,u_i} u_{i,F}^{(n)} + b_{P,u_i}^{(n-1)} - V_P \left(\frac{\partial p^{(n-1)}}{\partial x_i} \right)_P \right) + (1 - \alpha_{u_P}) u_{i,P}^{(n-1)} \quad (15a)$$

$$\text{and } u_{i,Q}^{(n)} = -\frac{\alpha_{u_Q}}{a_{Q,u_i}} \left(\sum_{F \in NB(Q)} a_{F,u_i} u_{i,F}^{(n)} + b_{Q,u_i}^{(n-1)} - V_Q \left(\frac{\partial p^{(n-1)}}{\partial x_i} \right)_Q \right) + (1 - \alpha_{u_Q}) u_{i,Q}^{(n-1)} \quad (15b)$$

where the superscript $(n-1)$ denotes the previous outer iteration number. The reader should note, that the pressure gradient has not been discretized yet. This has the advantage that the selective interpolation technique [?] can be applied, which is crucial for the elimination of the mentioned oscillations. In almost the same manner a semi-discrete implicit momentum can be formulated for a virtual control volume located between nodes P and Q (PICTURE)

$$u_{i,f}^{(n)} = -\frac{\alpha_{u_f}}{a_{f,u_i}} \left(\sum_{F \in NB(f)} a_{F,u_i} u_{i,F}^{(n)} + b_{f,u_i}^{(n-1)} - V_f \left(\frac{\partial p^{(n-1)}}{\partial x_i} \right)_f \right) + (1 - \alpha_{u_f}) u_{i,f}^{(n-1)} \quad (16)$$

To eliminate the artifacts surging form the virtualization of a control volume the following assumptions have to be made to derive a closed expression for the velocity on the boundary face S_f

$$\frac{\alpha_{u_f}}{a_{f,u_i}} \left(\sum_{F \in NB(f)} a_{F,u_i} u_{i,F}^{(n)} \right) \approx (1 - \gamma_f) \frac{\alpha_{u_P}}{a_{P,u_i}} \left(\sum_{F \in NB(P)} a_{F,u_i} u_{i,F}^{(n)} \right) + \gamma_f \frac{\alpha_{u_Q}}{a_{Q,u_i}} \left(\sum_{F \in NB(Q)} a_{F,u_i} u_{i,F}^{(n)} \right) \quad (17a)$$

$$\text{and } \frac{\alpha_{u_f}}{a_{f,u_i}} \approx (1 - \gamma_f) \frac{\alpha_{u_P}}{a_{P,u_i}} + \gamma_f \frac{\alpha_{u_Q}}{a_{Q,u_i}}, \quad (17b)$$

where γ_f is a geometric interpolation factor.

Using the assumptions made equation (17) the expression in equation (16) can be closed in a way that it only depends on the variable values in node P and Q

$$\begin{aligned}
u_{i,f}^{(n)} &\approx (1 - \gamma_f) \left(-\frac{\alpha_{u_P}}{a_{P,u_i}} \sum_{F \in NB(P)} a_{F,u_i} u_{i,F}^{(n)} \right) + \gamma_f \left(-\frac{\alpha_{u_Q}}{a_{Q,u_i}} \sum_{F \in NB(Q)} a_{F,u_i} u_{i,F}^{(n)} \right) \\
&\quad + \frac{\alpha_{u_f}}{a_{f,u_i}} b_{f,u_i}^{(n-1)} - \frac{\alpha_{u_f}}{a_{f,u_i}} V_f \left(\frac{\partial p^{(n-1)}}{\partial x_i} \right)_f + (1 - \alpha_u) u_{i,f}^{(n-1)} \\
&= (1 - \gamma_f) u_{i,P}^{(n)} - (1 - \gamma_f) \left(b_{Q,u_i}^{(n-1)} - V_Q \left(\frac{\partial p}{\partial x_i} \right)_Q^{(n-1)} \right) \\
&\quad + \gamma_f u_{i,Q}^{(n)} - \gamma_f \left(b_{Q,u_i}^{(n-1)} - V_Q \left(\frac{\partial p}{\partial x_i} \right)_Q^{(n-1)} \right) \\
&\quad + \frac{\alpha_{u_f}}{a_{f,u_i}} b_{f,u_i}^{(n-1)} - \frac{\alpha_{u_f}}{a_{f,u_i}} V_f \left(\frac{\partial p^{(n-1)}}{\partial x_i} \right)_f + (1 - \alpha_u) u_{i,f}^{(n-1)} \\
&= \left[(1 - \gamma_f) u_{i,P}^{(n-1)} + \gamma_f u_{i,Q}^{(n-1)} \right] \\
&\quad - \left[\left((1 - \gamma_f) \frac{\alpha_u V_P}{a_{P,u_i}} + \gamma_f \frac{\alpha_u V_Q}{a_{Q,u_i}} \right) \left(\frac{\partial p}{\partial x_i} \right)_f^{(n-1)} - (1 - \gamma_f) \frac{\alpha_u V_P}{a_{P,u_i}} \left(\frac{\partial p}{\partial x_i} \right)_P^{(n-1)} - \gamma_f \frac{\alpha_u V_Q}{a_{Q,u_i}} \left(\frac{\partial p}{\partial x_i} \right)_Q^{(n-1)} \right] \\
&\quad + (1 - \alpha) \left[u_{i,f}^{(n-1)} - (1 - \gamma_f) u_{i,P}^{(n-1)} - \gamma_f u_{i,Q}^{(n-1)} \right] \\
&\approx \left[(1 - \gamma_f) u_{i,P}^{(n-1)} + \gamma_f u_{i,Q}^{(n-1)} \right] \\
&\quad - \left((1 - \gamma_f) \frac{\alpha_u V_P}{a_{P,u_i}} + \gamma_f \frac{\alpha_u V_Q}{a_{Q,u_i}} \right) \left[\left(\frac{\partial p}{\partial x_i} \right)_f^{(n-1)} - (1 - \gamma_f) \left(\frac{\partial p}{\partial x_i} \right)_P^{(n-1)} - \gamma_f \left(\frac{\partial p}{\partial x_i} \right)_Q^{(n-1)} \right] \\
&\quad + (1 - \alpha) \left[u_{i,f}^{(n-1)} - (1 - \gamma_f) u_{i,P}^{(n-1)} - \gamma_f u_{i,Q}^{(n-1)} \right]. \tag{18}
\end{aligned}$$

It should be noted that the argumentation that led to the last expression is that the task of the pressure gradient corrector is to suppress oscillations. If there are no oscillations this part does not come into consideration. This is however true on equidistant grids, where $\gamma_f = \frac{1}{2}$. On grids with variation in the spacing one final modification has to be performed based on the following proposition.

PROPOSITION WITH PROOF

It is desirable for the pressure corrector to vanish if the profile of the pressure is quadratic. Using the following proposition this can be accomplished with modifying equation REFERENCE as

$$\begin{aligned}
u_{i,f}^{(n)} &= \left[(1 - \gamma_f) u_{i,P}^{(n-1)} + \gamma_f u_{i,Q}^{(n-1)} \right] \\
&\quad - \left((1 - \gamma_f) \frac{\alpha_u V_P}{a_{P,u_i}} + \gamma_f \frac{\alpha_u V_Q}{a_{Q,u_i}} \right) \left[\left(\frac{\partial p}{\partial x_i} \right)_f^{(n-1)} - \frac{1}{2} \left(\frac{\partial p}{\partial x_i} \right)_P^{(n-1)} - \frac{1}{2} \left(\frac{\partial p}{\partial x_i} \right)_Q^{(n-1)} \right] \\
&\quad + (1 - \alpha) \left[u_{i,f}^{(n-1)} - (1 - \gamma_f) u_{i,P}^{(n-1)} - \gamma_f u_{i,Q}^{(n-1)} \right]. \tag{19}
\end{aligned}$$

INTERPRET THE DIFFERENT TERMS OF THIS FINAL EQUATION

4.2 Implicit Pressure Correction and the SIMPLE Algorithm

The goal of finite volume methods is to deduce a system of linear algebraic equations from a partial differential equation. In the case of the momentum balances the general structure of this linear equations is

$$a_{P,u_i} u_{i,P}^{(n)} + \sum_{F \in NB(P)} a_{F,u_i} u_{i,F}^{(n)} = b_{P,u_i}^{(n)} - \left(\frac{\delta p^{(n)}}{\delta x_i} \right)_P, \tag{20}$$

where the pressure gradient has been discretized only symbolically and b_{p,u_i} denotes the source term. The symbolic discretization of the pressure gradient not only includes the discretization of the differential operator but, in the case a finite volume method is used, also the approximation of the integral. At this stage the equations are still coupled and non-linear. As described in section 3.4 the Picard iteration process will be used to linearize the equations. After this, every momentum balance equation will only depend on the one dominant variable u_i . Furthermore the coupling of the momentum balances through the convective term ($u_i u_j$) is resolved in the process of linearization. The decoupled momentum balances will then be solved sequentially for the dominant variable. All coefficients $a_{\{p,F\},u_i}$, the source term and the pressure gradient will be evaluated explicitly by using results of the preceding outer iteration ($n-1$) until the non-linear equations are fulfilled up to a certain tolerance (??). This leads to the following linear equation

$$a_{p,u_i} u_{i,p}^{(n*)} + \sum_{F \in NB(P)} a_{F,u_i} u_{i,F}^{(n*)} = b_{p,u_i}^{(n-1)} - \left(\frac{\delta p^{(n-1)}}{\delta x_i} \right)_p. \quad (21)$$

Here (*) indicates that the solution of this equation still needs to be corrected to also fulfill the discretized mass balance

$$\frac{\delta(\rho u_i^{(n)})}{\delta x_i} = 0. \quad (22)$$

The lack of an equation with the pressure as dominant variable leads to the necessity to alter the mass balance as the only equation left. Methods of this type are called projection methods. A common class of algorithms of this family of methods uses an equation for the additive pressure correction p' instead of the pressure itself and enforces continuity by correcting the velocities with an additive corrector u'_i :

$$u_{i,p}^{(n)} = u_{i,p}^{(n*)} + u'_{i,p}, \quad p_p^{(n)} = p_p^{(n-1)} + p'_p.$$

It is now possible to formulate the discretized momentum balance for the corrected velocities and the corrected pressure as

$$a_{p,u_i} u_{i,p}^{(n)} + \sum_{F \in NB(P)} a_{F,u_i} u_{i,F}^{(n)} = b_{p,u_i}^{(n-1)} - \left(\frac{\delta p^{(n)}}{\delta x_i} \right)_p. \quad (23)$$

It should be noted that the only difference between (23) and (20) is that the source term b_{p,u_i} has not been updated yet. To couple velocity and pressure correctors one can subtract equations (20) and (21) and consider the linearity of the discretization operator $\frac{\delta}{\delta x_i}$

$$u'_{i,p} = - \frac{\sum_{F \in NB(P)} a_{F,u_i} u'_{i,F}}{a_{p,u_i}} - \frac{1}{a_{p,u_i}} \left(\frac{\delta p'}{\delta x_i} \right)_p. \quad (24)$$

Since the global purpose of the presented method is to enforce continuity by implicitly calculating a pressure correction, the velocity correction has to be expressed in terms of the pressure correction and inserted into the discretized continuity equation (22) as follows

$$\left[\frac{\delta(\rho u_i^{(n*)})}{\delta x_i} \right]_p - \frac{\delta}{\delta x_i} \left[\frac{\sum_{F \in NB(P)} a_{F,u_i} u'_{i,F}}{a_{p,u_i}} \right]_p - \frac{\delta}{\delta x_i} \left[\frac{1}{a_{p,u_i}} \left(\frac{\delta p'}{\delta x_i} \right)_p \right]_p = \frac{\delta(\rho u_i^{(n*)})}{\delta x_i} + \frac{\delta(\rho u'_i)}{\delta x_i} = 0. \quad (25)$$

In order to separate the pressure correction p' , the dominant variable from the velocities the semi-discrete form of the pressure correction equation can be stated as

$$\frac{\delta}{\delta x_i} \left[\frac{1}{a_{p,u_i}} \left(\frac{\delta p'}{\delta x_i} \right)_p \right]_p = \left[\frac{\delta(\rho u_i^{(n*)})}{\delta x_i} \right]_p - \frac{\delta}{\delta x_i} \left[\frac{\sum_{F \in NB(P)} a_{F,u_i} u'_{i,F}}{a_{p,u_i}} \right]_p. \quad (26)$$

The majority of the class of pressure correction algorithms has this equation as common basis. Each algorithm then introduces special distinguishable approximations of the velocity corrections that are, at the moment of solving the pressure equation, still unknown and will be calculated by means of equation (24), after a solution to (26) has been obtained. The method used in the present work is the SIMPLE Algorithm (Semi-Implicit Method for Pressure-Linked Equations REFERENCE). The approximation this algorithm performs is severe since the term containing the unknown

velocity corrections is dropped entirely. The respective term has been underlined in (26) and accordingly in (24) for the velocity correction.

The approximation performed in the SIMPLE algorithm affects convergence in a way that the pressure correction has to be under-relaxed with a parameter $\alpha_p \in [0, 1]$

$$p_p^{(n)} = p_p^{(n-1)} + \alpha_p p'_p \quad (27)$$

The velocities will be under-relaxed as well for stability reasons. This will change the discrete momentum balance to

$$\frac{a_{p,u_i}}{\alpha_u} u_{i,p}^{(n)} + \sum_{F \in NB(P)} a_{F,u_i} u_{i,F}^{(n)} = b_{p,u_i}^{(n)} - \left(\frac{\delta p^{(n)}}{\delta x_i} \right)_p + \frac{(1 - \alpha_u)}{\alpha_u} u_{i,p}^{(n-1)},$$

A more detailed integration of the under-relaxation into the momentum balance will be found at the end of subsection (REFERENCE). The under-relaxation leads to an undesirable property of the SIMPLE algorithm, if the mass fluxes, to be introduced in subsection (REFERENCE), are calculated by the standard Rhie-Chow momentum interpolation scheme, which is the common practice. In this case the interpolation method will generate results that depend on the under-relaxation factor of the velocity α_u . Since the present work aims at a detailed comparison of the results of different solver algorithms an superior interpolation technique will be presented, namely the pressure weighted interpolation method.

Generally the SIMPLE algorithm can be represented by the following iterative procedure as in Algorithm 4.2.

Algorithm 1 SIMPLE Algorithm

Solve linearized momentum balances

$i = 1$

while $i \leq x.n$ and $k > x.key[i]$ **do**

▷ localize key

$i = i + 1$

end while

if $i \leq x.n$ **then**

▷ avoid array out of bounds

if $k == x.key[i]$ **then**

▷ check if key is in node

$inNode = true$

end if

end if

4.3 Discretization of the Momentum Balance

The stationary momentum balance integrated over a single control volume P reads as

$$\underbrace{\iint_S (\rho u_i u_j) n_j dS}_{\text{convective term}} - \underbrace{\iint_S \left(\mu \left(\frac{\partial u_i}{\partial x_j} + \frac{\partial u_j}{\partial x_i} \right) \right) n_j dS}_{\text{diffusive term}} = - \underbrace{\iiint_V \frac{\partial p}{\partial x_i} dV}_{\text{source term pressure}} - \underbrace{\iiint_V \rho \beta (T - T_0) dV}_{\text{source term temperature}} \quad (28)$$

where the different terms to be addressed individually in the following sections are indicated. Note that the form of this equation has been modified by using Gauss' integration theorem. The terms residing on the left will be treated in an implicit and due to deferred corrections in an explicit manner whereas the terms on the right will be treated exclusively in an explicit manner.

4.3.1 Linearization and Discretization of the Convective Term

The convective term $\rho u_i u_j$ of the Navier-Stokes equations is the reason for the non-linearity of the equations. In order to deduce a set of linear algebraic equations from the Navier-Stokes equations this term has to be linearized. As introduced in section (3.4), the non linearity will be dealt with by means of an iterative process, the Picard iteration. The part dependent on the non dominant dependent variable therefore will be approximated by its value from the previous iteration as $\rho u_i^{(n)} u_j^{(n)} \approx \rho u_i^{(n)} u_j^{(n-1)}$. However this linearization will not be directly visible because it will be covered by the mass flux $\dot{m}_f = \iint_{S_f} \rho u_j^{(n-1)} n_j dS$. Using the additivity of the Riemann integral the first step is to decompose the surface integral into individual contributions from each boundary face of the control volume P

$$\iint_S \rho u_i u_j n_j dS = \sum_{f \in \{w,s,b,t,n,e\}} \iint_{S_f} \rho u_i u_j n_j dS = \sum_{f \in \{w,s,b,t,n,e\}} F_{i,f}^c$$

where $F_{i,f}^c := \iint_{S_f} \rho u_i^{(n)} u_j^{(n-1)} n_j dS$ is the convective flux of the velocity u_i through the face S_f .

To improve diagonal dominance of the resulting linear system while maintaining the smaller discretization error of a higher order discretization, a blended discretization scheme is applied using a deferred correction. Since due to the non-linearity of the equations to be solved an iterative solution process is needed by all means, the overall convergence doesn't degrade noticeably when using a deferred correction. Blending and deferred correction result in a decomposition of the convective flux into a lower order approximation that is treated implicitly and the explicit difference between the higher and lower order approximation for the same convective flux. Since for coarse grid resolutions the use of higher order approximations may lead to oscillations of the solution which may degrade or even impede convergence, the schemes can be blended by a control factor $\eta \in [0, 1]$. To show the generality of this approach all further derivations are presented for the generic boundary face S_f that separates control volume P from its neighbour $F \in NB(P)$. This decomposition then leads to

$$F_{i,f}^c \approx \underbrace{F_{i,f}^{c,l}}_{\text{implicit}} + \eta \underbrace{[F_{i,f}^{c,h} - F_{i,f}^{c,l}]}_{\text{explicit}}^{(n-1)}.$$

Note that the convective fluxes carrying a l or h as exponent, already have been linearized and discretized. The discretization applied to the convective flux in the present work is using the midpoint integration rule and blends the upwind interpolation scheme with the linear interpolation scheme. Applied to above decomposition one can derive the following approximations

$$\begin{aligned} F_{i,f}^{c,l} &= u_{i,F} \min(\dot{m}_f, 0) + u_{i,P} \max(0, \dot{m}_f) \\ F_{i,f}^{c,h} &= u_{i,F} \gamma_f + u_{i,P} (1 - \gamma_f), \end{aligned}$$

where the variable values have to be taken from the previous iteration step $(n-1)$ as necessary and the mass flux \dot{m}_f has been used as result of the linearization process. The results can now be summarized by presenting the convective contribution to the matrix coefficients a_{F,u_i} and a_{P,u_i} and the right hand side b_{P,u_i} which are calculated as

$$a_{F,u_i}^c = \min(\dot{m}_f, 0), \quad a_{P,u_i}^c = \sum_{F \in NB(P)} \max(0, \dot{m}_f) \quad (29a)$$

$$\begin{aligned} b_{P,u_i}^c &= \sum_{F \in NB(P)} \eta \left(u_{i,F}^{(n-1)} (\min(\dot{m}_f, 0) - \gamma_f) \right) \\ &\quad + \eta \left(u_{i,P}^{(n-1)} (\max(0, \dot{m}_f) - (1 - \gamma_f)) \right) \end{aligned} \quad (29b)$$

4.3.2 Discretization of the Diffusive Term

The diffusive term contains the first partial derivatives of the velocity as result of the material constitutive equation that characterizes the behaviour of Newtonian fluids. As pointed out in section 3.3 directional derivatives can be discretized using central differences on orthogonal grids or in the more general case of non-orthogonal grids using central differences implicitly and a explicit deferred correction comprising the non-orthogonality of the grid. As seen in equation (7) the diffusive term of the Navier-Stokes equations can be simplified using the mass balance in the case of an incompressible flow with constant viscosity μ . To sustain the generality of the presented approach this simplification will be omitted.

As before, by using the additivity and furthermore linearity of the Riemann integral, the integration of the diffusive term will be divided into integration over individual boundary faces S_f

$$\iint_S \left(\mu \left(\frac{\partial u_i}{\partial x_j} + \frac{\partial u_j}{\partial x_i} \right) \right) n_j dS = \sum_{f \in \{w,s,b,t,n,e\}} \left[\iint_{S_f} \mu \frac{\partial u_i}{\partial x_j} n_j dS + \iint_{S_f} \mu \frac{\partial u_j}{\partial x_i} n_j dS \right] = \sum_{f \in \{w,s,b,t,n,e\}} F_{i,f}^d,$$

where $F_{i,f}^d$ denotes the diffusive flux through an individual boundary face. Section 3.3 only covered the non-orthogonal corrector for directional derivatives. Since the velocity is a vector field and not a scalar field, the results of section 3.3 may only be applied to the underlined term. The other term will be treated explicitly since it is considerably smaller than the underlined term and does not cause oscillations and thus will not derogate convergence. To begin with all present integrals will be approximated using the midpoint rule of integration. The diffusive flux $F_{i,f}^d$ for a generic face S_f then reads

$$F_{i,f}^d \approx \underbrace{\mu \left(\frac{\partial u_i}{\partial x_j} \right)}_{\text{implicit}} n_j S_f + \mu \left(\frac{\partial u_j}{\partial x_i} \right) n_j S_f.$$

Using central differences for the implicit discretization of the directional derivative and furthermore using the *orthogonal correction* approach from 3.3.2 the approximation can be derived as

$$\begin{aligned} F_{i,f}^d &\approx \mu \left(\frac{\|\Delta_f\|_2}{\|\mathbf{x}_P - \mathbf{x}_F\|_2} \frac{u_{P_i} - u_{F_i}}{\|\mathbf{x}_P - \mathbf{x}_F\|_2} - (\nabla u_i)_f^{(n-1)} \cdot (\Delta_f - \mathbf{S}_f) \right) + \mu \left(\frac{\partial u_j}{\partial x_i} \right)_f^{(n-1)} n_{f_i} \\ &= \mu \left(S_f \frac{u_{P_i} - u_{F_i}}{\|\mathbf{x}_P - \mathbf{x}_F\|_2} - \left(\frac{\partial u_i}{\partial x_j} \right)_f^{(n-1)} (\xi_{f_i} - n_{f_i}) S_f \right) + \mu \left(\frac{\partial u_j}{\partial x_i} \right)_f^{(n-1)} n_{f_i}, \end{aligned}$$

where the unit vector pointing in direction of the straight line connecting control volume P and control volume F is denoted as

$$\xi_f = \frac{\mathbf{x}_P - \mathbf{x}_F}{\|\mathbf{x}_P - \mathbf{x}_F\|_2}.$$

The interpolation of the cell center gradients to the boundary faces is performed as in (12). Now the contribution of the diffusive part to the matrix coefficients and the right hand side can be calculated as

$$a_{F,u_i}^d = -\frac{\mu S_f}{\|\mathbf{x}_P - \mathbf{x}_F\|_2}, \quad a_{P,u_i}^d = \sum_{F \in \text{NB}(P)} \frac{\mu S_f}{\|\mathbf{x}_P - \mathbf{x}_F\|_2} \quad (30a)$$

$$\begin{aligned} b_{F,u_i}^d &= \sum_{F \in \text{NB}(P)} \left(\frac{\partial u_i}{\partial x_j} \right)_f^{(n-1)} (\xi_{f_i} - n_{f_i}) S_f - \mu \left(\frac{\partial u_j}{\partial x_i} \right)_f^{(n-1)} n_{f_i} S_f \\ &= \left(\frac{\partial u_i}{\partial x_j} \right)_f^{(n-1)} \xi_{f_i} S_f - \mu \left(\left(\frac{\partial u_i}{\partial x_j} \right)_f^{(n-1)} - \left(\frac{\partial u_j}{\partial x_i} \right)_f^{(n-1)} \right) n_{f_i} S_f. \end{aligned} \quad (30b)$$

4.3.3 Discretization of the Source Terms

Since in the segregated solution approach in every equation all other variables but the dominant one are treated as constants and furthermore the source terms in equation (28) do not depend on the dominant variable the discretization is straightforward. The source terms of the momentum balance are discretized using the midpoint rule of integration, which leads to the source term

$$-\iiint_V \frac{\partial p}{\partial x_i} dV - \iiint_V \rho \beta (T - T_0) dV \approx -\left(\frac{\partial p}{\partial x_i} \right)_P^{(n-1)} V_P - \rho \beta (T_P^{(n-1)} - T_0) V_P = b_{P,u_i}^{sc} \quad (31)$$

4.4 Discretization of the Pressure Correction Equation

4.5 Discretization of the Temperature Equation

The discretization of the temperature equation is performed by the same means as for the momentum balance. The only difference is a simpler diffusion term. The integral form of the temperature equation after applying the Gauss' theorem of integration is

$$\underbrace{\iint_S \rho u_j T n_j dS}_{\text{advective term}} - \underbrace{\iint_S \kappa \frac{\partial T}{\partial x_j} n_j dV}_{\text{diffusive term}} = \underbrace{\iiint_V q_T dV}_{\text{source term}}.$$

Proceeding as in the previous subsections one can now discretize the advective, the diffusive term and the source term. Since this process does not provide further insight, just the final results will be presented. The discretization yields the matrix coefficients as

$$a_{F,T} = \min(\dot{m}_f, 0) + \frac{\kappa S_f}{\|\mathbf{x}_P - \mathbf{x}_F\|_2} \quad (32a)$$

$$a_{P,T} = \sum_{F \in NB(P)} \max(0, \dot{m}_f) - \frac{\kappa S_f}{\|\mathbf{x}_P - \mathbf{x}_F\|_2} \quad (32b)$$

$$\begin{aligned} b_{P,T} = & \sum_{F \in NB(P)} \eta \left(T_F^{(n-1)} (\min(\dot{m}_f, 0) - \gamma_f) \right) \\ & + \eta \left(T_P^{(n-1)} (\max(0, \dot{m}_f) - (1 - \gamma_f)) \right) \\ & + \sum_{F \in NB(P)} \left(\frac{\partial T}{\partial x_j} \right)_f^{(n-1)} (\xi_{f_j} - n_{f_j}) S_f \\ & + q_{T_P} V_P. \end{aligned} \quad (32c)$$

Again it is possible though not always necessary, as in the case of the velocities, to under-relax the solution of the resulting linear system with a factor α_T . This can be accomplished as shown in the previous sections.

4.6 Boundary Conditions

4.7 Structure of the Assembled Linear Systems

The objective of a finite volume method is to create a set of linear algebraic equations by discretizing partial differential equations. For the momentum balance all necessary components have been calculated. Taking all contributions together leads to the following linear algebraic equation for each control volume P

$$a_{P,u_i} u_{P_i} + \sum_{F \in NB(P)} a_F u_{F_i} = b_{P,u_i},$$

where the coefficients are composed as

$$a_{P,u_i} = a_{P,u_i}^c - a_{P,u_i}^d \quad (33)$$

$$a_{F,u_i} = a_{F,u_i}^c - a_{F,u_i}^d \quad (34)$$

$$b_{P,u_i} = b_{P,u_i}^c - b_{P,u_i}^d + b_{P,u_i}^{sc}. \quad (35)$$

In the case of control volumes located at boundaries some of the coefficients will be calculated in a different manner. This aspect will be addressed in a later section. For the decoupled iterative solution process of the Navier-Stokes equations it is necessary to reduce the change of each dependent variable in each iteration. Normally this is done by a *under-relaxation* technique, a convex combination of the solution of the linear system present iteration (n) and from the previous iteration ($n-1$) with the under-relaxation parameter α_{u_i} . Generally speaking this parameter can be chosen individually for each equation. Since there are no rules for choosing this parameters in a general setting the under-relaxation parameter for the velocities is chosen to be equal for all three velocities, $\alpha_{u_i} = \alpha_u$. This has the further advantage that, in case the boundary conditions are implemented with the same intention, the linear system for each of the velocities remains unchanged except for the right hand side. This helps to increase memory efficiency.

Let the solution for the linear system without under-relaxation be denoted as

$$\tilde{u}_{P_i}^{(n)} := \frac{b_{P,u_i} - \sum_{F \in NB(P)} a_F u_{F_i}}{a_{P,u_i}},$$

Which is only a formal expression. A convex combination as described yields

$$\begin{aligned} u_{P_i}^{(n)} &:= \alpha_u \tilde{u}_{P_i}^{(n)} + (1 - \alpha_u) u_{P_i}^{(n-1)} \\ &= \alpha_u \frac{b_{P,u_i} - \sum_{F \in NB(P)} a_F u_{F_i}}{a_{P,u_i}} + (1 - \alpha_u) u_{P_i}^{(n-1)}, \end{aligned}$$

an expression that can be modified to derive a linear system whose solution is the under-relaxed velocity

$$\frac{a_{p,u_i}}{\alpha_u} u_{i,p} + \sum_{F \in NB(p)} a_{F,u_i} u_{i,F} = b_{p,u_i} + \frac{(1 - \alpha_u) a_{p,u_i}}{\alpha_u} u_{i,p}^{(n-1)}.$$

It must be noted that under-relaxation has not been accounted for in the derivation of the Rhie-Chow interpolation method (REFERENCE). As it has been shown the results depend on the choice of the under-relaxation factor. However under-relaxation is necessary for overall convergence, so in order to be able to compare the results of the different solver algorithms this dependency has to be eliminated. Subsection (REFERENCE) will present a common approach to resolve this dependency.

5 Finite Volume Method for Incompressible Flows – Coupled Approach

Since the antecedent section already discussed the discretization of the momentum balance the focus of this section will be on highlighting the differences and presenting various approaches to incorporate different degrees of velocity-temperature and temperature-velocity/pressure coupling. It should be noted that the discretization of the equations to be solved is not changed in any way, so the presented differences only are due to difference in the solution algorithm. As in the previous section the final forms of the presented equations are presented as they are implemented in the developed solver framework.

5.1 The Coupled Algorithm

5.1.1 Pressure Equation

5.1.2 Characteristic Properties of Coupled Solution Methods

No Underrelaxation needed, higher memory requirements

Bad condition, singularity, usually faster convergence if efficient linear solver is chosen, coupling in Buoyancy flows (s.a. Peric page 448, Galpin Raithby) Design of algorithm does not need to enforce continuity (is inherently fulfilled because of the coupling of the equations)

Explicitly mention the differences

- Implicit treatment of Pressure Gradient
- Implicit Treatment of Temperature possible
- Boussinesq approximation brings velocity-to-temperature-coupling (vakilipour), Newton-Raphson Linearization
- Temperature dependent densities also possible

5.2 Coupling the Temperature Equation

5.2.1 Decoupled Approach

5.2.2 Velocity-Temperature Coupling

5.2.3 Temperature-Velocity/Pressure Coupling – Newton-Raphson Linearization

5.3 Boundary Conditions on Domain and Block Boundaries

5.3.1 Dirichlet Boundary Condition for Velocity

5.3.2 Wall Boundary Condition

5.3.3 Block Boundary Condition

5.4 Assembly of Linear Systems – Final Form of Equations

6 CAFFA Framework

CAFFA is an acronym and stands for Computer Aided Fluid Flow Analysis. Based on Peric `caffa 2d` code, 3 dimensional extension to blockstructured grids. Characteristic is the parallelisation with PETSc and the fully implicit treatment of arbitrary block boundaries.

6.1 PETSc Framework

PETSc is an acronym for Portable Extensible Toolkit for Scientific Calculations and is a software library. Keep in mind not to copy the manual

6.1.1 About PETSc

Bell Prize, MPI Programming

6.1.2 Basic Data Types

Vec, Mat (Different Matrix Types and Their effect on complex methods)

6.1.3 KSP and PC Objects and Their Usage

Singularities

6.1.4 Profiling

PETSc Log

6.1.5 Common Errors

Optimization, Interfaces, (ROWMAJOR, COLUMNMAJOR), Compiler Errors not helpful, Preallocation vs. Mallocs

6.2 Grid Generation and Conversion

Generation of block structured locally refined grids with non-matching block interfaces, neighbouring relations are represented by a special type of boundary conditions; Random number generator to move grid points within a epsilon neighbourhood while maintaining the grid intact. Show in a graph how preallocation impacts on runtime.

6.3 Preprocessing

Matching algorithm – the idea behind clipper and the used projection technique; alt.: Opencascade. Efficient calculation of values for discretization. Important for dynamic mesh refinement, arbitrary polygon matching, parallelizable due to easier interface

6.4 Implementation Details of CAFFA

6.4.1 MPI Programming Model

Basic idea of distributed memory programming model, emphasize the differences to shared memory model. Have a diagram at hand that shows how CAFFA sequentially works (schedule) and point out the locations where and of which type (global reduce, etc.) communication is, or when synchronization is necessary.

- after each solve
- pressure reference
- error calculation
- gradient calculation

Point out that one should try to minimize the number of this points such that parallel performance stays high. Better to calculate Velocity and Pressure Gradients at once not by separately calling this routine.

6.4.2 Convergence Control

Explain how the criterion for convergence is met

6.4.3 Modi of Calculation

there are different modi of calculation, (NS segregated, then scalar; NS and Scalar Segregated; NS coupled and Scalar segregated; Fully coupled (watch out with fully coupled, this term seems to have already another meaning)). Note that for comparison of solvers it is crucial to develop programs on the same basis. This establishes comparability.

6.4.4 Indexing of Variables and Treatment of Boundary Values

Describe MatZeroValues and how it is used to simplify the code. Also loose a word on PCREDISTRIBUTE its advantages (no boundary values involved, do not have to be reset when system is solved with high tolerance) and downsides (preliminary tests showed bad scaling behaviour (PROVE)). Compliance of PETSc zero based indexing and CAFFA indexing which considers boundary values.

6.4.5 Field Interlacing

Realization through special arrangement of variables and the use of index sets (subvector objects) and/or preprocessor directives. Advantages (there was a paper I cited in my thesis). Note that not all variables are interlaced (Velocities are, but their gradients are not). Great impact on Matrix structure.

6.4.6 Domain Decomposition, Exchange of Ghost Values and Parallel Matrix Assembly

- Ghost values are stored in local representations of the global vector (state the mapping for those entries).
- Matrix coefficients are calculated on one processor and sent to the neighbour.
- Preallocation as crucial aspect for program performance. For the coupled system the matrix is assembled in a 2-3 step process to save memory for coefficients.
- Present a simple method for balancing the matrix related load by letting PETSc take care of matrix distribution.
- Use Spy function of Matlab to visualize the sparse matrices. Point out advantages of calculating coefficients for the neighbouring cells locally (no need to update mass fluxes, geometric data doesn't need to be shared, small communication overhead since processors assemble matrix parts that don't belong to them (visualize)).
- Paradigm: Each time new information is available perform global updates. Advantages of using matrices: Show structure of matrix when using arbitrary matching vs. higher memory requirements vs. better convergence

6.5 Postprocessing

Visualization of Results with Paraview and Tecplot Export matrices as binaries and visualize them using matlab scripts.

7 Verification of the developed CAFFA Framework

Different parts, describe incremental approach, only present final results. Refer to next section for Validation of CAFFA

7.1 Theoretical Discretization Error

present the Taylor-Series Expansion

7.2 Method of Manufactured Solutions

basically sum up the important points of salari's technical report, symmetry of solution/domain/grid is bad point out that mms is not able to detect errors in the physical model Also loose a word or two about discontinuous manufactured solutions

7.3 Exact and Manufactured Solutions for the Navier-Stokes Equations and the Energy Equation

Not always there is an exact solution. Divergence free approach. Presentation of the used manufactured solution. What if solution is not divergence free? Derivation of equations and modifications to continuity equation. analyze the problem of too complicated manufactured solutions. also use temperature dependent density function. Explain why global mass conservation in a discrete sense is important and how it can be achieved. Special domain, vanishing manufactured solution or symmetric manufactured solutions if a higher approximation of boundary fluxes is not feasible.

- <http://scicomp.stackexchange.com/questions/6943/manufactured-solutions-for-incompressible-navier-stokes>
- <http://link.springer.com/article/10.1007/BF00948290>
- <http://physics.stackexchange.com/questions/60476/exact-solutions-to-the-navier-stokes-equations>
- <http://www.annualreviews.org/doi/pdf/10.1146/annurev.fl.23.010191.001111>

7.4 Measurement of Error and Calculation of Order

Different error measures (L2-Norm, completeness of function space, consistency etc.)

7.4.1 Testcase on Single Processor on Orthogonal Locally Refined Grid

7.4.2 Testcase on Multiple Processors on Non-Orthogonal Locally Refined Grid

Give a measure of the grid quality.

8 Comparison of Solver Concepts

8.1 Convergence Behaviour on Locally Refined Block Structured Grids with Different Degrees of Coupling

Show how the implicit treatment of block boundaries maintains (high) convergence rates. Plot Residual over number of iterations.

8.2 Parallel Performance

8.2.1 Employed Hardware and Software – The Lichtenberg-High Performance Computer

- Networking
- Mem Section and processes in between islands (calculating across islands)
- Versioning information (PETSc, INTEL COMPILERS, CLIPPER, MPI IMPLEMENTATION, BLAS/LAPACK)
- Software not designed to perform well on desktop PCs.

8.2.2 Measures of Performance

- Maße definieren
- Nochmal Hager, Wellein studieren
- Guidelines for measuring performance (bias through system processes or user interaction), only measure calculation time do not consider I/O in the beginning and the end
- Cite Schäfer and Peric with their different indicators for parallel efficiency, load balancing and numerical efficiency

8.2.3 Preliminary Upper Bounds on Performance – The STREAM Benchmark

Pinning of processes (picture), preliminary constraints by hardware and operating systems, identification of bottlenecks and explain possible workarounds, history and results of STREAM. Bandwidth as Bottleneck, how to calculate a Speedup estimate based on the measured bandwidth. PETSc Implementation of STREAM

8.2.4 Discussion of Results for Parallel Efficiency

8.2.5 Speedup Measurement for Analytic Test Cases

8.3 Test Cases with Varying Degree of Non-Linearity

As Peric says I want to prove that the higher the non-linearity of NS, the better relative convergence rates can be achieved with a coupled solver. Fi

8.3.1 Transport of a Passive Scalar – Forced Convection

8.3.2 Buoyancy Driven Flow – Natural Convection

8.3.3 Flow with Temperature Dependent Density – A Highly Non-Linear Test Case

Maybe I could consider two test cases, one with oscillating density and one with a quadratic polynomial. Interesting would be also to consider the dependence of convergence on another scalar transport equation

8.4 Realistic Testing Scenarios – Benchmarking

Also consider simple load balancing by distributing matrix rows equally

8.4.1 Flow Around a Cylinder 3D – Stationary

Describe Testing Setup (Boundary conditions and grid). Present results and compare them with literature.

8.4.2 Flow Around a Cylinder 3D – Instationary

- http://www.featflow.de/en/benchmarks/cfdbenchmarking/flow/dfg_flow3d/dfg_flow3d_configuration.html

Describe Testing Setup (Boundary conditions and grid). Present results and compare them with literature.

8.4.3 Heat-Driven Cavity Flow

- http://www.featflow.de/en/benchmarks/cfdbenchmarking/mit_benchmark.html

Describe Testing Setup (Boundary conditions and grid). Present results and compare them with literature.

8.5 Realistic Testing Scenario – Complex Geometry

9 Conclusion and Outlook

Turbulence (turbulent viscosity has to be updated in each iteration), Multiphase (what about discontinuities), GPU-Accelerators, Load-Balancing, dynamic mesh refinement, Conjugate Heat Transfer with other requirements for the numerical grid, grid movement, list some papers here) Identify the optimal regimes / conditions for maximizing performance. Each solver concept has its strengths and weaknesses. Try other variants of Projection Methods like SIMPLEC, SIMPLER, PISO or PIMPLE (OpenFOAM)

References

- [1] BALAY, S., ABHYANKAR, S., ADAMS, M. F., BROWN, J., BRUNE, P., BUSCHELMAN, K., ELJKHOUT, V., GROPP, W. D., KAUSHIK, D., KNEPLEY, M. G., MCINNES, L. C., RUPP, K., SMITH, B. F., AND ZHANG, H. PETSc users manual. Tech. Rep. ANL-95/11 - Revision 3.5, Argonne National Laboratory, 2014.
- [2] BALAY, S., ABHYANKAR, S., ADAMS, M. F., BROWN, J., BRUNE, P., BUSCHELMAN, K., ELJKHOUT, V., GROPP, W. D., KAUSHIK, D., KNEPLEY, M. G., MCINNES, L. C., RUPP, K., SMITH, B. F., AND ZHANG, H. PETSc Web page. <http://www.mcs.anl.gov/petsc>, 2014.
- [3] BALAY, S., GROPP, W. D., MCINNES, L. C., AND SMITH, B. F. Efficient management of parallelism in object oriented numerical software libraries. In *Modern Software Tools in Scientific Computing* (1997), E. Arge, A. M. Bruaset, and H. P. Langtangen, Eds., Birkhäuser Press, pp. 163–202.
- [4] CHEN, Z., AND PRZEKWAŚ, A. A coupled pressure-based computational method for incompressible/compressible flows. *Journal of Computational Physics* 229, 24 (2010), 9150 – 9165.
- [5] CHOI, S. K. Note on the use of momentum interpolation method for unsteady flows. *Numerical Heat Transfer, Part A: Applications* 36, 5 (1999), 545–550.
- [6] CHOI, S.-K., KIM, S.-O., LEE, C.-H., AND CHOI, H.-K. Use of the momentum interpolation method for flows with a large body force. *Numerical Heat Transfer, Part B: Fundamentals* 43, 3 (2003), 267–287.
- [7] CHRISTON, M. A., GRESHO, P. M., AND SUTTON, S. B. Computational predictability of time-dependent natural convection flows in enclosures (including a benchmark solution). *International Journal for Numerical Methods in Fluids* 40, 8 (2002), 953–980.
- [8] DARWISH, M., SRAJ, I., AND MOUKALLED, F. A coupled finite volume solver for the solution of incompressible flows on unstructured grids. *Journal of Computational Physics* 228, 1 (2009), 180 – 201.
- [9] FALK, U., AND SCHÄFER, M. A fully coupled finite volume solver for the solution of incompressible flows on locally refined non-matching block-structured grids. In *Adaptive Modeling and Simulation 2013* (Barcelona, Spain, June 2013), J. P. M. de Almeida, P. Diez, C. Tiago, and N. Parež, Eds., pp. 235–246.
- [10] GALPIN, P. F., AND RAITHBY, G. D. Numerical solution of problems in incompressible fluid flow: Treatment of the temperature-velocity coupling. *Numerical Heat Transfer* 10, 2 (1986), 105–129.
- [11] GALPIN, P. F., AND RAITHBY, G. D. Numerical solution of problems in incompressible fluid flow: Treatment of the temperature-velocity coupling. *Numerical Heat Transfer* 10, 2 (1986), 105–129.
- [12] GRESHO, P. M., AND SANI, R. L. On pressure boundary conditions for the incompressible navier-stokes equations. *International Journal for Numerical Methods in Fluids* 7, 10 (1987), 1111–1145.
- [13] HUI, W. Exact solutions of the unsteady two-dimensional navier-stokes equations. *Journal of Applied Mathematics and Physics ZAMP* 38, 5 (1987), 689–702.
- [14] JASAK, H. *Error Analysis and Estimation for the Finite Volume Method with Applications to Fluid Flows*. PhD thesis, Imperial College of Science, Technology and Medicine, Jun 1996.
- [15] KUNDU, P. K., COHEN, I. M., AND DOWNLING, D. R. *Fluid Mechanics*, 5 ed. Elsevier, 2012.
- [16] LI, W., YU, B., WANG, X.-R., AND SUN, S.-Y. Calculation of cell face velocity of non-staggered grid system. *Applied Mathematics and Mechanics* 33, 8 (2012), 991–1000.
- [17] MAJUMDAR, S. Role of underrelaxation in momentum interpolation for calculation of flow with nonstaggered grids. *Numerical Heat Transfer* 13, 1 (1988), 125–132.
- [18] MILLER, T. F., AND SCHMIDT, F. W. Use of a pressure-weighted interpolation method for the solution of the incompressible navier-stokes equations on a nonstaggered grid system. *Numerical Heat Transfer* 14, 2 (1988), 213–233.
- [19] PERIC, M. Analysis of pressure-velocity coupling on nonorthogonal grids. *Numerical Heat Transfer* 17 (Jan. 1990), 63–82.

-
- [20] RAMAMURTI, R., AND LÖHNER, R. A parallel implicit incompressible flow solver using unstructured meshes. *Computers & Fluids* 25, 2 (1996), 119 – 132.
- [21] RHIE, C. M., AND CHOW, W. L. Numerical study of the turbulent flow past an airfoil with trailing edge separation. *AIAA Journal* 21 (Nov. 1983), 1525–1532.
- [22] SALARI, K., AND KNUPP, P. Code verification by the method of manufactured solutions. Tech. Rep. SAND2000-1444, Sandia National Labs., Albuquerque, NM (US); Sandia National Labs., Livermore, CA (US), Jun 2000.
- [23] SCHÄFER, M., AND TUREK, S. Recent benchmark computations of laminar flow around a cylinder, 1996.
- [24] SHEU, T. W. H., AND LIN, R. K. Newton linearization of the incompressible navier–stokes equations. *International Journal for Numerical Methods in Fluids* 44, 3 (2004), 297–312.
- [25] VAKILIPOUR, S., AND ORMISTON, S. J. A coupled pressure-based co-located finite-volume solution method for natural-convection flows. *Numerical Heat Transfer, Part B: Fundamentals* 61, 2 (2012), 91–115.
- [26] VAN DOORMAAL, J. P., AND RAITHBY, G. D. Enhancements of the simple method for predicting incompressible fluid flows. *Numerical Heat Transfer* 7, 2 (1984), 147–163.
- [27] ZHANG, S., ZHAO, X., AND BAYYUK, S. Generalized formulations for the rhie–chow interpolation. *Journal of Computational Physics* 258, 0 (2014), 880 – 914.